Journal of The Electrochemical Society, **156** (7) D236-D241 (2009)
0013-4651/2009/156(7)/D236/6/$25.00 © The Electrochemical Society

Improvement in the Oxidation Resistance of Cu Films by an Electroless Co-Alloy Capping Process

Hyo-Chol Koo,[a] Sung Ki Cho,[a] Oh Joong Kwon,[b] Myung-Won Suh,[c] Young Im,[c] and Jae Jeong Kim[a,*,z]

[a]*School of Chemical and Biological Engineering, Seoul National University, Seoul 151-744, Korea*
[b]*Department of Mechanical Engineering, University of Incheon, Incheon 402-749, Korea*
[c]*KC Tech Company, Limited, Kyonggi 456-843, Korea*

Co-alloy films with various solution compositions [CoB, CoWB, and CoW(B)P] were deposited with an electroless technique on Cu films without Pd activation, and their oxidation barrier performance was analyzed. The degrees of oxidation of all films were intensively studied. CoB showed excellent capping performance as an oxidation barrier, whereas CoWB and CoW(B)P exhibited even poorer oxidation resistance than the case of bare Cu at 400°C. The depth profile of the film compositions and chemical states of the CoB film before and after oxidation was investigated, the results of which suggested that the oxidation of the B component in the film had a clear role in the prevention of continuous Cu diffusion to the surface. The multilayer structure of CoB/CoW(B)P/Cu for obtaining both electromigration and oxidation resistance was optimized, showing excellent oxidation resistance comparable to a single-composition CoB film.
 [DOI: 10.1149/1.3133219]

Manuscript submitted December 11, 2008; revised manuscript received February 16, 2009. Published May 15, 2009.

In the fabrication of Cu metal lines using the damascene process in ultralarge-scale integration technology, the upper Cu surface exposed after a chemical mechanical polishing (CMP) process must be shielded with a diffusion barrier. Dielectric materials such as SiN_x and SiC_xN_y have been used for this purpose, and these are deposited on the whole substrate without a selective etching process. However, the dielectric constants of these materials are higher than those of the low-*k* materials used for the interlevel dielectric, which leads to an increase in the effective dielectric constant between the metal lines and the increment in resistor–capacitor delays.[1] Furthermore, a continuous increase in integrity has promoted an increase in the current density of the metal lines, which induces serious electromigration issues.[2] It has been reported that the high interfacial energy between metallic–dielectric interfaces (Cu–dielectric capping layer) is the region where the electromigration phenomenon occurs.[2,3]

Electroless deposition of a thin Co-based alloy film on top of the exposed Cu metal line is the most promising solution to these problems.[4] Selective electroless deposition of Co-alloy layers, which act as diffusion barriers, also reduces the total volume of the capping layer and therefore decreases the effective dielectric constant of the entire metal line structure.[1] Furthermore, the interface of the Cu–Co alloy is metal–metal, which may have a lower interfacial energy than the previous metal–dielectric construction. This scheme significantly increases the lifetime of the metal line and also clearly increases the activation energy for the interfacial diffusion of Cu.[5]

Capping layers based on Co or Ni with the addition of boron or phosphorus during electroless deposition have been widely researched for various applications, including wear-resistive coating and magnetic materials. These capping layers have also included further ternary refractory alloy metals such as tungsten or molybdenum. The incorporation of boron or phosphorus is known to result from the chemical reduction of reducing agents.[6] Boron, phosphorus, and tungsten are considered to be elements capable of blocking the diffusion of Cu at the grain boundary of Co or Ni, thereby playing a vital role as a diffusion barrier.[7] Recent studies showed that the addition of a small amount of dimethylamine borane (DMAB) induces Pd-free electroless deposition on a Cu surface from a CoWP electrolyte, whereas using only hypophosphite requires Pd activation to deposit an alloy film.[8]

Another property that is expected to improve with the electroless capping process is the oxidation resistance of the Cu line. Cu does not form a self-passivation layer like Al, and continuous oxidation occurs when it is exposed to an oxidizing environment. The formation of an oxide layer between Cu and the diffusion barrier interface increases the effective resistivity of the metal line and is also a major cause of the electromigration phenomenon. In previous studies, an improvement in the oxidation properties was mainly achieved by the injection of alloy elements during the deposition of Cu, which diffused to the surface to form a permanent passivation layer.[9,10] In previous research, our group showed that a thin Ag layer deposited by a displacement reaction with Cu enhanced the oxidation resistance of Cu.[11] Also, the insertion of Ag ions during the CMP process resulted in the deposition of a very thin and smooth Ag capping layer with good oxidation resistance.[12] In those studies, the growth mechanism of the Cu oxide was the continuous diffusion of Cu to the surface. Recently, it was reported that the CoB film had better oxidation resistance than other Co-based capping layers.[13]

In this paper, capping layers, including CoW(B)P, CoWB, and CoB, deposited by electroless deposition without Pd activation on a Cu substrate were studied. Their performance as an oxidation barrier was tested, and their properties related to oxidation resistance are discussed.

Experimental

In this study, 500 nm thick Cu films were electrodeposited on a 60 nm thick Cu seed layer (by physical vapor deposition) with a Ta/TaN (15/15 nm) diffusion barrier on p-type Si(100) wafers used as substrates. All of the depositions were performed on 1.5 cm square-shaped samples. Before electroless deposition, the Cu native oxide was removed by dipping the sample in a solution containing citric acid and KOH for 2 min. The electroless deposition process was performed at 70°C. The detailed solution compositions are listed in Table I. Three types of capping layers with different compositions were used; each film was referred to according to its composition as CoB, CoWB, or CoW(B)P. We assumed that the addition of each component into the solution would deposit each alloy ele-

Table I. Composition of the electroless deposition bath (unit: M).

	CoB	CoWB	CoW(B)P
$CoSO_4 \cdot 7H_2O$	0.07	0.07	0.07
$Na_3C_6H_5O_7$	0.46	0.46	0.46
NaOH	0.66	0.66	0.66
H_3BO_3	1.0	1.0	1.0
$Na_2WO_4 \cdot 2H_2O$	—	0.076	0.076
5-aminotetrazole	—	0.0004	0.001
$NaH_2PO_2 \cdot H_2O$	—	—	0.23
DMAB	0.12	0.12	0.01

* Electrochemical Society Active Member.
z E-mail: jjkimm@snu.ac.kr

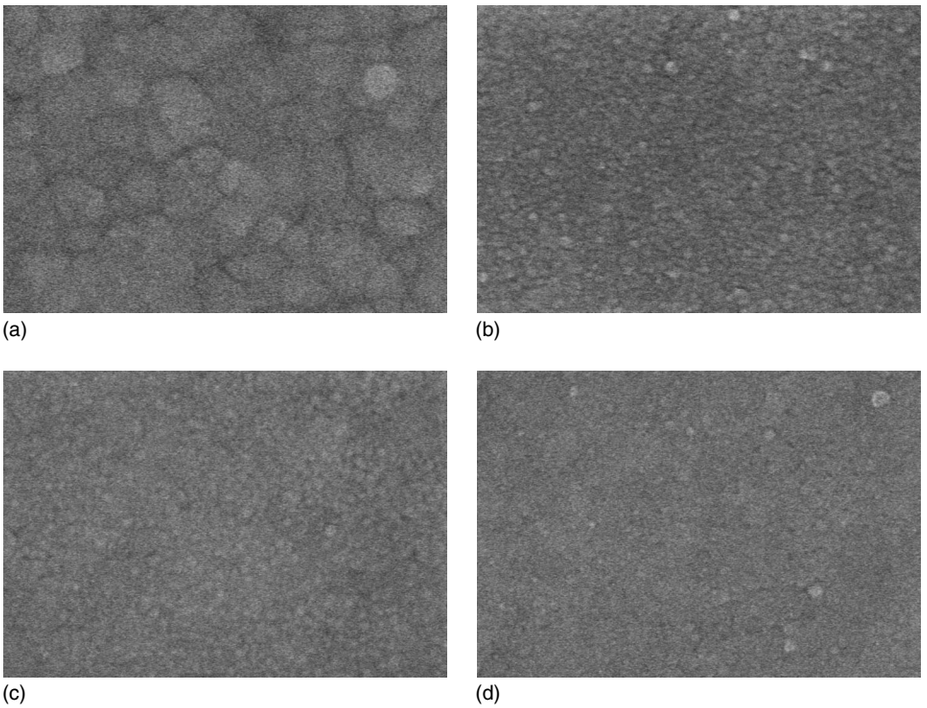

Figure 1. Surface morphologies of Co-alloy films deposited on Cu surfaces: (a) CoP on Pd-activated Cu, (b) CoW(B)P film on Cu without activation, (c) CoWB on Cu, and (d) CoB on Cu.

ment, i.e., boron from DMAB, phosphorus from hypophosphite, and tungsten from sodium tungstate, as reported previously.[6] The use of the parentheses in the designation CoW(B)P indicated the minor component in the capping layer due to the addition of a very small amount of DMAB compared to sodium hypophosphite. Because the thickness of the CoWP film without the addition of DMAB on Pd-activated Cu was about 19 nm after 12 min deposition through transmission electron microscope analysis, we assumed that the thickness of the capping layers on Cu without Pd activation was similar or slightly thicker.

The oxidation of the samples was performed in a horizontal quartz-tube furnace that had been purged with N_2 gas (99.999%) while increasing and decreasing the furnace temperature to inhibit unwanted oxidation. The temperature ramp rate was 16.7°C/min, and cooling occurred mainly by natural convection. During oxidation at a targeted temperature, the air pressure was controlled at about 1 atm by the addition of filtered compressed air. All of the samples were loaded on an alumina boat, and the edges of the samples were sealed by Kapton tape to direct oxidation only in the direction normal to the surface.

The surface morphologies of the samples were observed by field-emission-scanning electron microscopy (FESEM), and depth profiles of the samples after oxidation were analyzed using Auger electron spectroscopy (AES). The detailed chemical state of each element and the changes in composition after oxidation were identified from X-ray photoelectron spectroscopy (XPS).

Results and Discussion

The surface morphologies are shown in Fig. 1. The films were very smooth and defect-free in all cases. Grooves on the surface were rarely observed on the CoB surface, whereas the CoWB surface showed distinguishable grooves. For the CoP film deposited on Pd-activated Cu, grains distinguished by grooving were relatively

Table II. Composition of the deposited films analyzed by AES.

	Co	W	B	P	O
CoWB	72.1	15.5	—	—	7.4
CoW(B)P	74.2	1.3	1.4	12.1	4.9
CoB	64.7	—	18.4	—	10.2

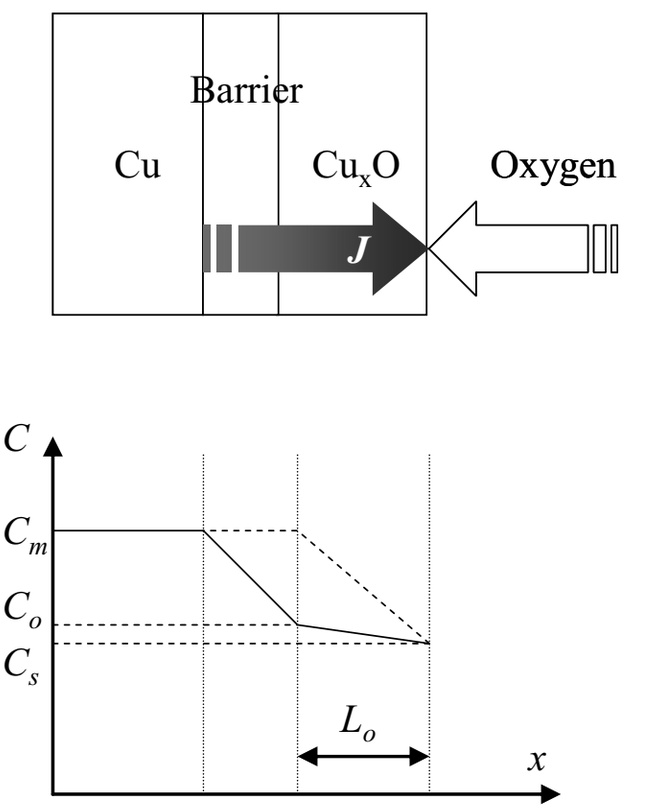

Figure 2. Schematic diagram of an oxidation model for a Cu film with capping layer.

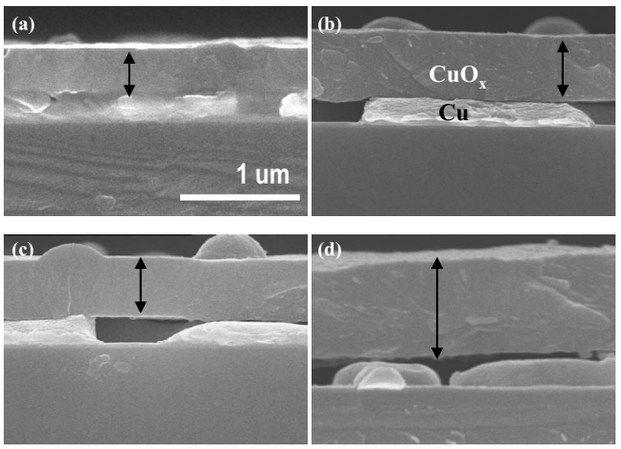

Figure 3. Cross-sectional FESEM images of the Cu film after oxidation: after (a) 4, (b) 9, (c) 16, and (d) 25 min.

large compared to the other cases. These differences might result from the high nucleation density on the continuous Cu surface, which acts as a catalyst for electroless deposition compared to the discontinuous Pd clusters in the CoP case.

The compositions of the films are listed in Table II. All films contained 65–75 atom % Co, with various concentrations of boron, phosphorus, tungsten, and oxygen. The oxygen composition was a few percent, except in the CoB film, which had over 10% oxygen. When tungstate ions were added to the electrolyte for CoWB deposition, the composition difference between CoWB and CoB was notable;[13] CoB had almost 20% boron, whereas CoWB had no detectable boron peaks based on AES analysis. The tungsten concentration in CoWB was about 15%, which suggested that the deposition of tungsten and boron was competitive. For CoW(B)P, the concentration of boron and tungsten was quite small compared to that of phosphorus.

In this research, the changes in sheet resistance of the films were used to measure the degree of oxidation because the reciprocal of the sheet resistance is linearly dependent on the thickness when the resistivity of the film is constant and close in value to the bulk resistivity (over a 100 nm range). Assuming that oxidized Cu is completely nonconductive, the ratio of the Cu film thickness consumed by the oxidation process to the original thickness can be used as a quantitative term to represent the progress of the oxidation process. A simplified model for explaining the oxidation process is depicted in Fig. 2. During oxidation, the consumption rate of the Cu film at the surface must be equal to the amount of Cu that diffused through the Cu–oxide layer. This assumption must also apply when there is a capping layer that decelerates the diffusion of Cu.

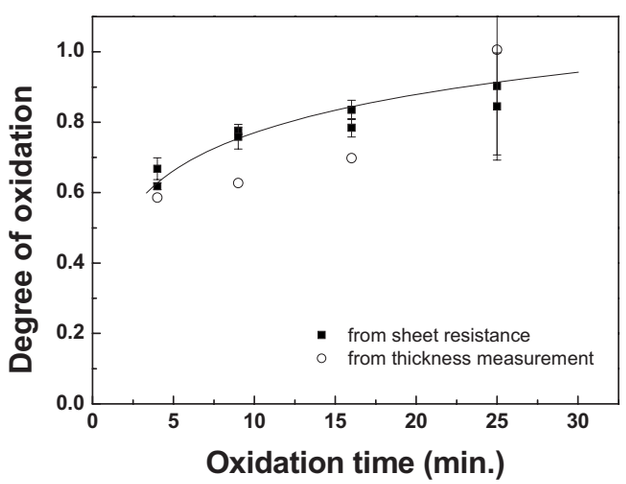

Figure 4. Changes in the degree of oxidation of Cu films without capping, calculated from the sheet resistance (black squares) and from the measurement of oxide thickness (white circles).

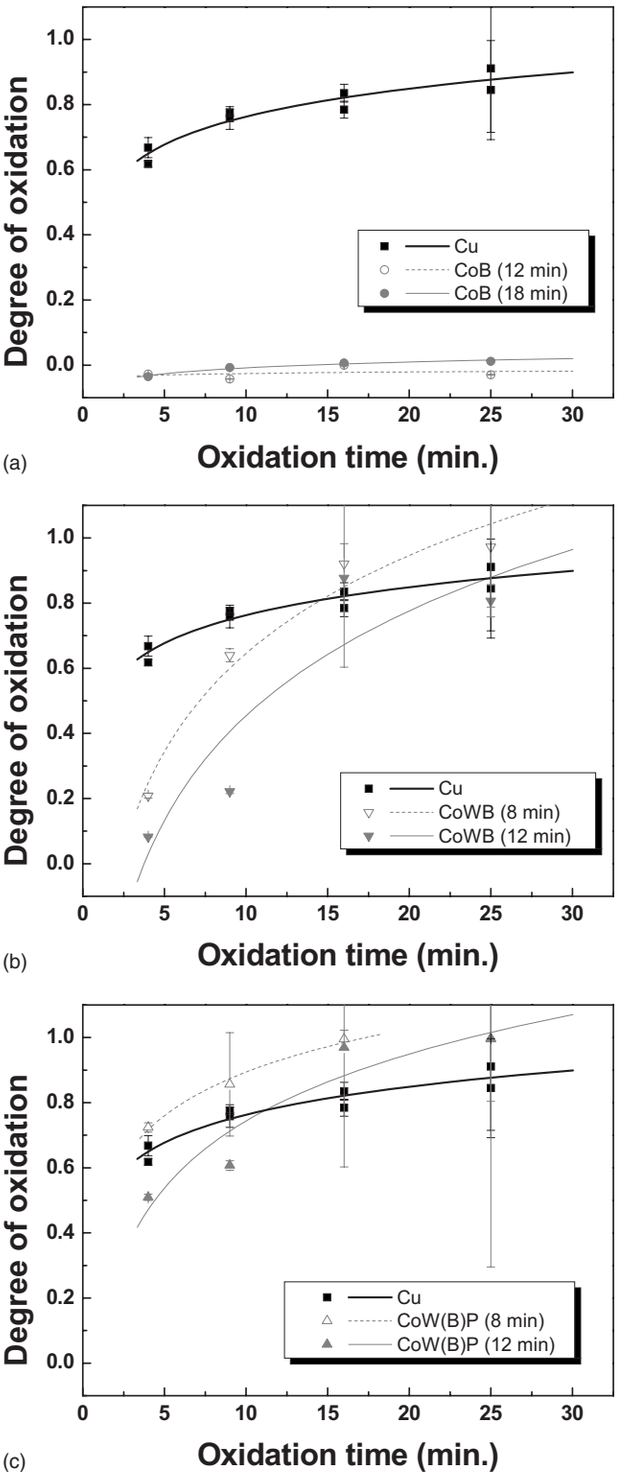

Figure 5. Changes in the degree of oxidation of Cu films with capping layers and their thicknesses: (a) CoB, (b) CoWB, and (c) CoW(B)P.

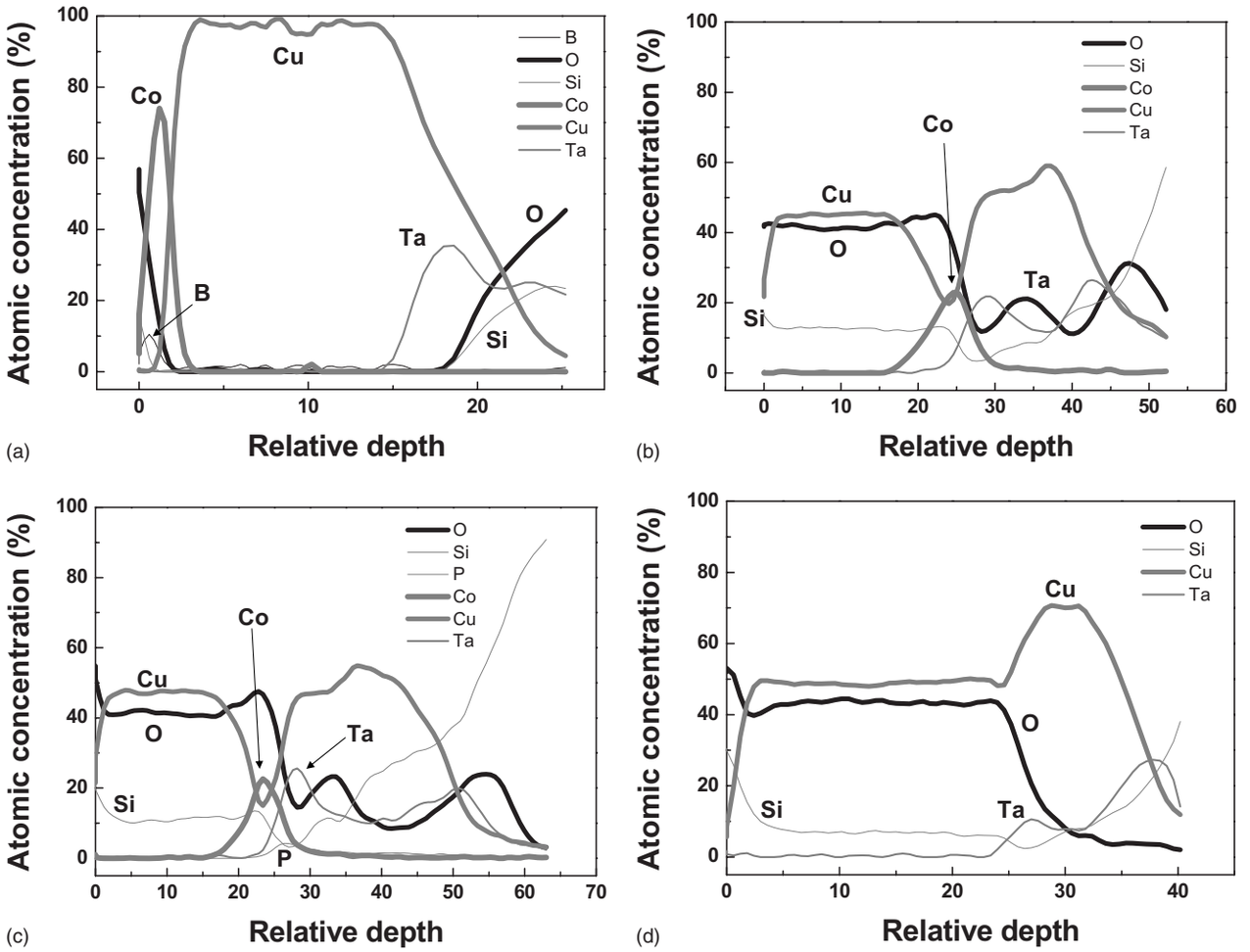

Figure 6. AES depth profiles of Cu films with capping layers after oxidation at 400°C for 25 min: (a) CoB (18 min deposition), (b) CoWB (12 min deposition), (c) CoW(B)P (12 min deposition), and (d) Cu film without capping.

Assuming a pseudo-steady-state isotropic diffusion through the oxide, a uniform consumption rate of Cu, a very fast oxidation reaction rate at the surface of the oxide (only mass-transfer-limited reaction), and a homogeneous Cu–oxide density, the governing equation of the system can be simplified as follows

$$J = D_o \frac{dC}{dx} = D_o \frac{C_o - C_s}{L_o} = k \frac{dL_o}{dt} \quad [1]$$

where J represents the total flux of Cu to the surface, D_o is the diffusion coefficient of Cu in the oxide, C_o is the concentration of Cu at the Cu–oxide interface, C_s is the concentration of Cu on the oxide surface, L_s is the thickness of the oxide film, and k is the Cu consumed per unit thickness of oxide film formed.

By rearranging Eq. 1

$$L_o = \sqrt{\frac{2D_o}{k}(C_o - C_s)}\sqrt{t} \quad [2]$$

one can see that the thickness of the oxide layer is proportional to the root of the oxidation time. If a capping layer exists (Fig. 2), Cu must undergo two diffusion steps through both the capping layer and the Cu oxide, and the equation is transformed as follows

$$\frac{1}{2}L_o^2 = \frac{1}{k}\left(\frac{D_c L_o}{L_c + \frac{D_c}{D_o}L_o}(C_m - C_s)\right)t \approx \frac{D_c}{k}\left(\frac{L_o}{L_c}(C_m - C_s)\right)t \quad [3]$$

where C_m represents the concentration of Cu at the capping layer–metal interface, D_c is the diffusion coefficient of Cu in the capping layer, and L_c is the thickness of the capping layer. If the capping layer strongly inhibits the diffusion of Cu ($D_c \ll D_o$), Eq. 3 can be expressed in the previous form, and a linear relationship between oxide thickness and oxidation time can be obtained

$$L_o = \frac{2D_c}{k}\left(\frac{1}{L_c}(C_m - C_s)\right)t \quad [4]$$

As shown in Fig. 3, Cu films oxidized at 400°C revealed that the consumption of Cu was not uniform, and very large holes formed below the upper Cu–oxide film. This may be due to agglomeration and void formation at high temperatures originating from the unstable interface between Cu and Cu oxide. As a result, the thicknesses of the remaining Cu films were slightly different in terms of the degree of oxidation, as calculated from the changes in sheet resistance shown in Fig. 4. However, overall trends were similar between values obtained from the measurement of the oxide thickness and the degree of oxidation calculated from the sheet resis-

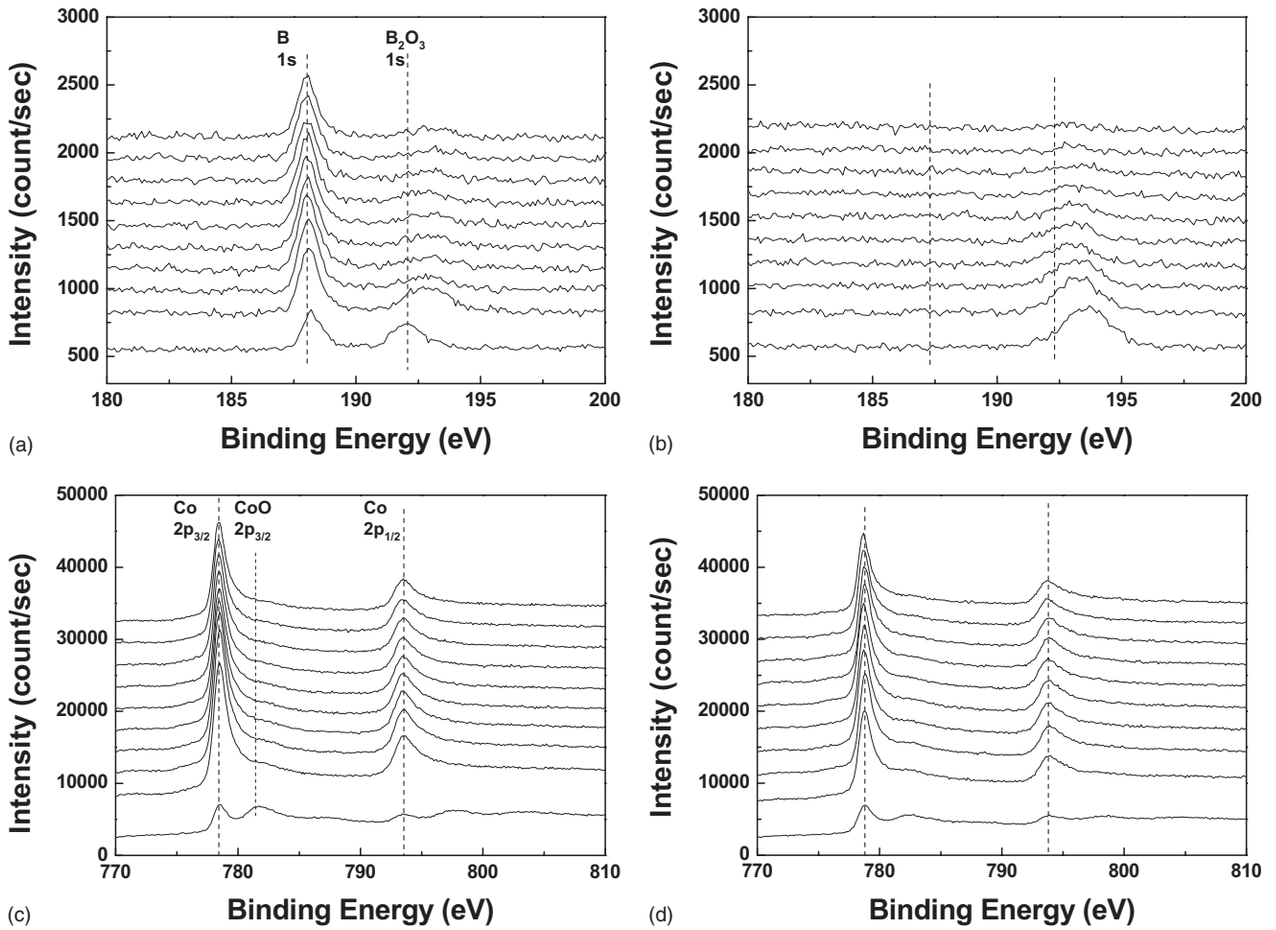

Figure 7. XPS depth profile of CoB layers: boron peaks (a) before and (b) after oxidation, and Co peaks (c) before and (d) after oxidation. The oxidation conditions were at 400°C for 25 min in atmospheric condition. The bottom of the graph represents the surface.

tance. Therefore, all of the values for the degree of oxidation in this paper were calculated from the changes in the sheet resistance.

Figure 5 depicts the changes in sheet resistances after oxidation with variations in the capping layer. The Cu film with CoB capping showed no obvious changes in sheet resistance. There was no significant difference between the uncapped Cu film and the CoWB and CoW(B)P capped Cu films except for the short oxidation time of the CoWB/Cu structure. The slight decrease in the resistance after the oxidation of CoB could be attributed to the annealing effect of the fully protected Cu layer by the capping layers. Even though thicker capping layers in CoWB and CoW(B)P had better oxidation resistance, complete oxidation was inevitable with longer oxidation times. Overall oxidation trends followed the predicted relationship of the square-root dependency of the oxidation time, which means that CoWB and CoW(B)P do not prevent Cu film oxidation.

The composition depth profiles, measured by AES on the films after oxidation with the capping layers, are shown in Fig. 6. CoB protected the Cu films completely from oxidation and the out-diffusion of Cu, and enabled the weak penetration of oxygen into the capping layer. However, as expected, films without any capping showed thick Cu–oxide layers on top of the film. The composition of Cu oxide was uniform throughout the oxide thickness; the oxide was likely in the form of CuO, considering the atomic ratio of Cu and oxygen. The CoWB and CoW(B)P capping layers were not effective in hindering Cu film oxidation (Fig. 6b and c). Though the capping layer itself remained without any redistribution or mixing with the copper film, copper oxide layers formed on the upper side of the capping layers, suggesting that the Cu atoms diffused easily through the capping layer. This resulted in the continuous formation of the oxide. The concentration of Cu was low in the capping layer (Co-rich) region, which might be due to the low solid solubility of Cu in a Co matrix,[14] whereas the oxygen concentration in the Co-rich region did not show an obvious decrease. Due to the low solubility of Cu in Co, most Cu atoms were expelled through the grain boundaries of the Co capping layers. Though it was not clear whether the diffusion of oxygen through the capping layer was suppressed or not, it was obvious that a large amount of oxygen did diffuse and resided in the capping layer itself, as shown in the figures. Dual-peak distributions of Ta, oxygen, and Si were observed deeper in the capping layers, which might be caused by the formation of large holes below the oxide layers. All these results supported the initial assumption that oxide layer formation was from the out-diffusion of Cu atoms through the capping layers and oxide layers.

For a more precise analysis of the CoB capping layer resistance to oxidation, the depth profile and chemical state of CoB before and after oxidation were analyzed by XPS. Before oxidation, the amount of boron in the film was over 30%, which is very large compared to previously observed compositions of boron in the CoB film.[13] Pure boron and B_2O_3 were detected, but the composition of pure boron was almost double that found in B_2O_3. There was about 10% oxygen within the film, which was mainly due to boron oxide (Fig. 7a). After oxidation, the concentration of boron decreased slightly, and a substantial portion of boron diffused out close to the surface. Most of the boron had been oxidized (Fig. 7b), whereas there were no

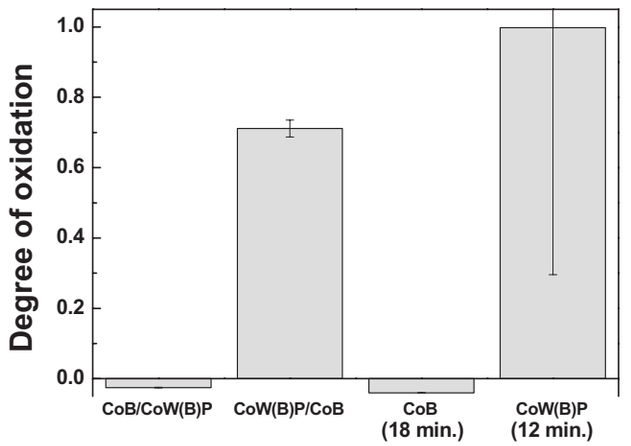

Figure 8. Changes in the degree of oxidation of the Cu film with multilayer capping films and single capping films. The deposition conditions of multilayer capping films were CoB (9 min)/CoW(B)P (6 min)/Cu and CoW(B)P (6 min)/CoB (9 min)/Cu, respectively.

significant changes in the chemical state of Co (Fig. 7c and d). These results revealed that during oxidation, the prevalent oxidized species was boron, not Co, with some redistribution of the chemical composition. It is assumed that such oxidation and redistribution of boron may be the key parameter in blocking the out-diffusion of Cu. Specifically, the enlargement of boron atoms due to the formation of B_2O_3, usually located on the grain boundaries of the Co matrix, will strongly block the diffusion path. However, it is not apparent why only boron acted as a blocking element, whereas phosphorus and tungsten did not have similar results in CoWB and CoW(B)P. In other cases, the diffusion of Cu might be due to the oxidation of the capping layers, which was supported by the distribution of oxygen and Co shown in Fig. 6. Furthermore, other studies have mentioned that the existence of tungsten damaged the oxidation resistance of the film for CoWB,[13] which was also observed in this research.

From these results, a double-layered capping process is proposed. It is well known that electromigration is strongly inhibited by the CoWP capping layer, which may result from its strong adhesion (and lower interfacial energy) to Cu.[15] CoB showed good oxidation resistance, and our experiments suggested that this was due to the oxidation of the CoB film, especially boron. Therefore, it is expected that a double-layer cap with a CoB/CoW(B)P/Cu structure will have excellent resistance to both electromigration and the oxidation of Cu. Furthermore, Co demonstrates catalytic activity in the electroless deposition bath with both DMAB and hypophosphite; thus, any additional catalyzation processes may not be required in double-layered capping.

Figure 8 shows that the oxidation resistance of the CoB/CoW(B)P/Cu structure with similar total thickness was excellent, similar to the case for CoB. However, the reverse structure capping layer [CoW(B)P/CoB/Cu] showed poor oxidation resistance. With CoW(B)P on the top of the structure, the oxygen diffusion through the capping layer is suppressed, which prevents the formation of blocking components (possibly boron oxide) in the CoB capping layer. Previous results in AES depth profiles have revealed that the capping layers, which are unable to prevent the oxidation of Cu layers, might themselves suppress the diffusion of oxygen. This result confirms our assumption that component oxidation near the CoB surface performs well as an oxidation barrier and also suggests a solution for controlling the performance of the capping layer by mixing two or more different films.

Conclusions

Co-based capping layers were formed by electroless deposition on Cu without Pd activation. CoB showed excellent resistance to the oxidation of Cu; almost no changes in sheet resistance or the depth profile were detected, even at oxidation conditions of 400°C for 25 min. CoB also completely protected the lower Cu film from oxidation or out-diffusion. Other capping layers, including CoWB and CoW(B)P, did not protect the lower copper film efficiently, allowing both the out-diffusion of copper through the capping layer and the formation of an oxide layer. The CoB oxidation resistance performance may originate from the oxidation of CoB itself, especially the oxidation of boron components near the surface. The double-layered capping layer [CoB/CoW(B)P/Cu] also inhibited Cu oxidation, whereas reverse structure capping did not show comparable oxidation resistance. This result supports the idea that the specific oxidation of Co is a decisive process for improving the oxidation resistance of the Cu film. Therefore, CoB promises to provide excellent resistance to both electromigration and oxidation of Cu film.

Acknowledgments

This research was supported by the Nano R&D program through the Korea Science and Engineering Foundation (KOSEF), which is funded by the Ministry of Education, Science and Technology (no. 2008-02857), and by the KOSEF through the Research Center for Energy Conversion and Storage (RCECS).

Seoul National University assisted in meeting the publication costs of this article.

References

1. ITRS Roadmap, 2007 edition.
2. C.-K. Hu, R. Rosenberg, and K. Y. Lee, *Appl. Phys. Lett.*, **74**, 2945 (1999).
3. C.-K. Hu, L. M. Gignac, E. Linger, C. Detavenier, S. G. Malhotra, and A. Simon, *J. Appl. Phys.*, **98**, 124501 (2005).
4. C.-K. Hu, L. M. Gignac, R. Rosenberg, B. Herbst, S. Smith, J. Rubino, D. Canaperi, S. T. Chen, S. C. Seo, and D. Restaino, *Appl. Phys. Lett.*, **84**, 4986 (2004).
5. T. L. Tan, C. L. Gan, A. Y. Du, C. K. Cheng, and J. P. Gambino, *Appl. Phys. Lett.*, **92**, 201916 (2008).
6. A. Kohn, M. Eizenberg, Y. Shacham-Diamand, and Y. Sverdlov, *Mater. Sci. Eng., A*, **302**, 18 (2001).
7. A. Kohn, M. Eizenberg, Y. Shacham-Diamand, B. Israel, and Y. Sverdlov, *Microelectron. Eng.*, **55**, 297 (2001).
8. H. Nakano, T. Itabashi, and H. Akahoshi, *J. Electrochem. Soc.*, **152**, C163 (2005).
9. P. J. Ding, W. A. Lanford, S. Hymes, and S. P. Murarka, *Appl. Phys. Lett.*, **64**, 2897 (1994).
10. P. J. Ding, W. A. Lanford, S. Hymes, and S. P. Murarka, *J. Appl. Phys.*, **75**, 3627 (1994).
11. J. J. Kim, Y. S. Kim, and S.-K. Kim, *Electrochem. Solid-State Lett.*, **6**, C17 (2003).
12. M. C. Kang, Y. J. Kim, and J. J. Kim, *Electrochem. Solid-State Lett.*, Submitted.
13. H. Einati, V. Bogush, Y. Sverdlov, Y. Rosenberg, and Y. Shacham-Diamand, *Microelectron. Eng.*, **82**, 623 (2005).
14. R. H. Yu, X. X. Zhang, M. Knobel, and P. Tiberto, *Scr. Metall. Mater.*, **33**, 2045 (1995).
15. M. W. Lane, E. G. Liniger, and J. R. Lloyd, *J. Appl. Phys.*, **93**, 1417 (2003).